Estuaries and Coasts Vol. 30, No. 4, p. 698–709 August 2007

Modeling of the Cape Fear River Estuary Plume

MENG XIA[1,*], LIAN XIE[1], and LEONARD J. PIETRAFESA[2]

[1] *Department of Marine, Earth and Atmospheric Sciences, North Carolina State University, P. O. Box 8208, Raleigh, North Carolina 27695*

[2] *College of Physical and Mathematical Sciences, North Carolina State University, P. O. Box 8208, Raleigh, North Carolina 27695*

ABSTRACT: The Environmental Fluid Dynamic Code, an estuarine and coastal ocean circulation model, is used to simulate the distribution of the salinity plume in the vicinity of the mouth of the Cape Fear River Estuary, North Carolina. The individual and coupled effects of the astronomical tides, river discharge, and atmospheric winds on the spatial and temporal distributions of coastal water levels and the salinity plume were investigated. These modeled effects were compared with water level observations made by the National Oceanic and Atmospheric Administration and salinity surveys conducted by the Coastal Ocean Research and Monitoring Program. Model results and observations of salinity distributions and coastal water level showed good agreement. The simulations indicate that strong winds tend to reduce the surface plume size and distort the bulge shape near the estuary mouth due to enhanced wind-induced surface mixing. Under normal discharge conditions, tides, and light winds, the southward outwelling plume veers west. Relatively moderate winds can mechanically reverse the flow direction of the plume. Under conditions of weak to moderate winds the water column does not mix vertically to the bottom, while in strong wind cases the plume becomes vertically well mixed. Under conditions of high river discharge the plume increases in size and reaches the bottom. Vertical mixing induced by strong spring tides can also enable the plume to reach the bottom.

Introduction

The freshwater discharge from the Cape Fear River, the Northeast Cape Fear River, and the Black River converges in the Cape Fear Estuary and flows into Long Bay as an outwelling salinity plume (33°54′N, 78°W). The average combined discharge from these rivers is about 221 $m^3 s^{-1}$ (Dame et al. 2000), with a maximum of about 2,000 $m^3 s^{-1}$. The relatively fresh plume of the Cape Fear River Estuary (CFRE) reduces salinity and modifies other water properties, such as temperature, nutrients, and phytoplankton, in the adjacent coastal ocean, affecting the water quality and sediment structure of the total local ecosystem (Mallin et al. 2005).

River-derived freshwater discharging into an adjacent continental shelf generally forms a trapped river plume that propagates to its right in the Northern Hemisphere in a narrow region along the coast due to the effect of the Earth's rotation (Zhang et al. 1987). Using satellite imagery, field observations, and models, additional factors such as tides, winds, strength of vertical stratification, and bottom topography have been found by previous investigations to influence the orientation and structure of river plumes (Hickey et al. 1998; Xie and Pietrafesa 1999; Xing and Davies 1999; Walker et al. 2005).

*Corresponding author; tele: 919/513-2025; fax: 919/515-1683; e-mail: mxia@ncsu.edu

Chao and Boicourt (1986) showed that vertical mixing induces much stronger seaward transport at the mouth of Chesapeake Bay. Fong and Geyer (2002) found that freshwater discharges from Chesapeake and Delaware Bays create a predominantly freshwater signature toward the right and downstream of the bay mouths. Zhang et al. (1987), Hickey et al. (1998), and Fong and Geyer (2002) found that upwelling favorable winds tend to move the plume water offshore while downwelling favorable winds reinforce the natural outwelling mode and further pin the plume to the coastline. Light winds were found to have minor effects on plume orientation, while moderate to strong winds were found to be capable of fully reversing the plume and changing its structure (Zhang et al. 1987; Kourafalou et al. 1996a). Astronomical tides greatly influence the plume structure, especially the vertical salinity distribution as discussed by Cheng and Casulli (2004). Tidal currents also contribute significantly to the total kinetic energy in the shelf and nearshore regions (Kourafalou et al. 1996b).

Over the past two decades there have been a series of analytical and numerical studies that have attempted to simulate plume formation and subsequent time and space history. Chao and Boicourt (1986) and Chao (1988) used a three-dimensional, primitive-equation model to simulate the onset of plumes. Zhang et al. (1987) used a nontidal theoretical model to simulate the various orientations of outwelled plumes. Garvine (1987) used a layered model to simulate an estuary plume by

including the effect of the Coriolis force. Garvine (1999, 2001) used a three-dimensional numerical model, ECOM3d, and conducted numerous experiments to denote the distribution of a plume on an idealized continental shelf. O'Donnell (1990) modeled the formation of a river plume by using a mathematical model. Kourafalou et al. (1996a, b) modeled the Savannah River plume. Sheng (2001) examined the nonlinear dynamics of a buoyancy-driven coastal current and estuarine plume using a z-level ocean model. Berdeal et al. (2002) used ECOM3d to simulate the high river discharge plume in the Columbia River. Cheng and Casulli (2004) and Baptista et al. (2005) used the unstructured grid model to simulate the dynamical processes of plumes in general.

There is extensive and robust literature on plume modeling, but there are significant limitations in all of these prior studies. Ideal geometry and physical settings were used. Due to the lack of observational data in the plume region, the results of most of those studies could only be validated using limited observations; e.g., salinity observations are in general lacking and could not be used for model validation. A detailed description of the vertical plume structure under the influence of various physical environmental conditions is lacking.

In this study, the Environmental Fluid Dynamic Code (EFDC) is used to simulate the CFRE plume and investigate the sensitivity of the plume to wind, river discharge, and tidal effects. Xia et al. (2006) used EFDC to simulate the surface structure of the CFRE plume. In the present study, the model domain is enlarged to allow the generation of wind-induced currents in the region surrounding the plume, avoiding some of the lateral boundary effects. The effects of astronomical tides were not considered in Xia et al. (2006). The present study extends that of Xia et al. (2006) in three aspects: both surface and vertical plume structures are considered, a higher resolution domain is used in the plume region to resolve the details of the three-dimensional plume near the mouth of the estuary, and the effects of wind, river discharge, and tides are considered separately and collectively. The EFDC model is briefly described and calibrated here. Ideal plume simulation experiments and results also are presented.

Model Description and Configuration

A Brief Description of the EFDC Model

The numerical model used in this study is based on a general purpose three-dimensional hydrodynamic model, EFDC (Hamrick 1992). The physics of the EFDC model and many aspects of the computational scheme resemble the Blumberg-Mellor model (Blumberg and Mellor 1987) that has been widely used for estuarine and coastal modeling (Ji et al. 2001; Shen and Haas 2004; Park et al. 2005; Yang and Hamrick 2005).

The following are the main reasons that we selected the EFDC model in this study. An embedded turbulence closure submodel (Mellor and Yamada 1982; Galperin et al. 1988) for parameterizing vertical turbulence mixing is included in the model. The use of sigma coordinates (Blumberg and Mellor 1987) in the model is well suited to study the near surface structure of plumes. The model includes the anti-diffusion upwind advection scheme that is more suitable for the plume study than the upwind scheme or the central difference scheme (Berdeal et al. 2002). EFDC uses orthogonal curvilinear or Cartesian horizontal coordinates in the grid generation, which allows the grid size to be variable in order to fit the coastlines of the river and estuary. Another important reason for selecting the EFDC model is that it includes sediment and water quality simulation submodels, which will be used for future CFRE plume studies.

In the simulations of the CFRE plume, 11 sigma layers were used in the vertical dimension. As Berdeal et al. (2002) pointed out, sufficient vertical resolution is important for plume modeling. Since freshwater plumes are confined to the near surface waters of the upper coastal ocean, finer levels were used near the free surface, while more coarse vertical levels were used closer to the bottom in the model. An orthogonal curvilinear grid was used in the model simulation with higher resolution in the river proper, estuary, and river mouth to resolve the complex coastline. There are a total of 1,895 grid cells in the relatively complex domain. The grid size varies from 100 m to 10 km within the model domain. Since horizontal resolution is critical for plume simulations (Fong 1998), higher resolution grids were generated near the mouth of CFRE and the plume region. The model also includes an efficient mode-splitting technique. The time step is set to 60 s to satisfy the Courant-Friedrich-Levy criterion. The bathymetry is derived from the National Geophysical Data Center Coastal Relief Model Volume 02 (Fig. 1).

River Discharge Settings

The Cape Fear River watershed in North Carolina consists of the Cape Fear, Black, and Northeast Cape Fear Rivers. For retrospective simulations, sources for field data used in the modeling study were obtained from United States Geological Survey stream flow gages in the rivers. Based on these data, the daily averaged Cape Fear River discharge is 158 $m^3 s^{-1}$ and the maximum historical river discharge is 1,618 $m^3 s^{-1}$. For the Black River, the daily

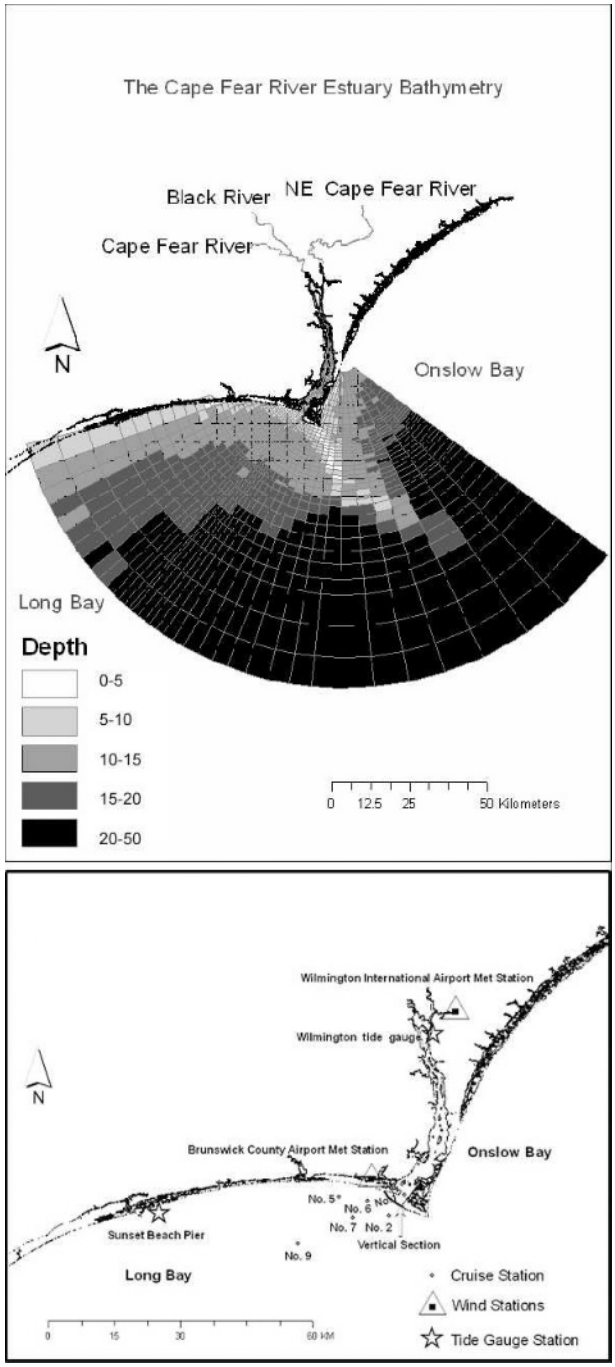

Fig. 1. The grids and bathymetry in the Cape Fear River Estuary modeling domain and locations of cruise and wind stations and tide gauges.

averaged river discharge and the historical maximum discharge are 23 and 773 $m^3 s^{-1}$, respectively. The corresponding discharges from the Northeast Cape Fear River are 20 and 847 $m^3 s^{-1}$, respectively. These observed data are the bases for setting river discharges for sensitivity studies.

Tides

Three semidiurnal constituents (M2, S2, N2) and two diurnal constituents (K1, O1) were used to simulate the tides in the model. The open boundary conditions were specified in keeping with the harmonic constants of the five major tidal constituents using tide datum (http://www.marine.unc.edu/C_CATS/tides/tides.htm) (Table 1). The data from Sunset Beach Pier and the Wilmington Gauge were obtained from the National Oceanic and Atmospheric Administration (NOAA). The Sunset Beach Pier site was deployed as part of the NOAA sponsored Carolinas Coastal Ocean Observations and Prediction Program.

Wind Forcing

The model domain is confined to the continental shelf area since the CFRE plume does not extend beyond the shelf break. The wind data used in the simulation are from the Wilmington International Airport and Brunswick County Airport stations (Fig. 1). Model sensitivity experiments used surface wind stress calculated from the well-known relationship

$$(\tau_{xz}, \tau_{yz}) = (\tau_{sx}, \tau_{sy}) = c_s\sqrt{U_W^2 + V_W^2}(U_W, V_W) \quad (1)$$

with U_W and V_W being the x and y components of the wind velocity with the drag coefficient c_s based on Wu (1982):

$$c_s = 0.001\frac{\rho_a}{\rho_w}\left(0.8 + 0.065\sqrt{U_w^2 + V_w^2}\right) \quad (2)$$

with ρ_a and ρ_w denoting air and water densities, respectively.

Salinity and Temperature Fields

The salinity and temperature fields in the CFRE undergo considerable seasonal variability, with lower values in the winter and higher values in the summer. The initial salinity and temperature of the river and estuary were set in keeping with values measured in the Lower Cape Fear River Program, while continental shelf water was initialized using data from Coastal Ocean Research and Monitoring Program's (CORMP) shipboard monitoring survey. At the open boundary, the salinity was set at a constant (36.5 psu) while daily sea temperature changes were based on the observations collected as part of the CORMP sampling program. A five-day spin-up was used in all experiments to allow for thermodynamic adjustment in the model.

The Simulation of the March 22, 2005 Case

On March 22, 2005, a shipboard survey was conducted to collect salinity data at designated

TABLE 1. Illustrative tidal constituents at the open boundary and in the model domain. Note: Amplitudes are in meters; Phases are in degrees, referenced to UTC (GMT).

		Open Boundary							
		Amplitude		Phase		Sunset Beach Pier		Wilmington Gauge	
Name	Period(s)	Max	Min	Max	Min	Amplitude	Phase	Amplitude	Phase
M2	44714.16	0.75	0.51	348.98	352.53	0.72	355.90	0.63	63.10
S2	43200.00	0.13	0.09	10.41	5.96	0.12	13.10	0.08	97.70
N2	45570.05	0.17	0.11	334.83	339.52	0.17	339.00	0.13	51.00
K1	86164.09	0.12	0.09	183.74	180.66	0.09	188.90	0.08	229.80
O1	92949.62	0.09	0.07	196.51	193.82	0.07	196.10	0.06	233.50

CFRE stations (Fig. 1). During that period, river discharge values were near average. The plume model simulation of this case was used for testing model sensitivity. Xia et al. (2006) employed the EFDC to verify simulated water levels under the conditions of no river discharge and no wind. The simulated tides and constructed tides show good agreement in the CFRE and adjacent coastal ocean.

With the five tidal constituents as well as the river discharge and wind effects considered, the model was used to simulate water level and salinity trends. Time-series data for the surface elevation were obtained by using tide gauges at the two stations from the NOAA (www.co-ops.noaa.gov): Wilmington Gauge and Sunset Beach Pier (Fig. 1). The comparison of simulated water level and observation data was plotted in Fig. 2. From this comparison, the simulated and observed water levels show good agreement. Correlation coefficients are 0.92 for Sunset Pier and 0.91 for Wilmington Gauge with an average absolute error of 0.17 and 0.16 m, respectively.

In the March 22, 2005 survey, the salinity values were collected for six cruise stations, which cover most of the plume region (Fig. 1). The model-calculated salinity was compared with measured data at the six stations (Fig. 3). The line represents the simulated salinity value near each station, while the point value represents the observational data. The model simulation appears to provide a reasonable reproduction of the observed salinity in the CFRE plume region.

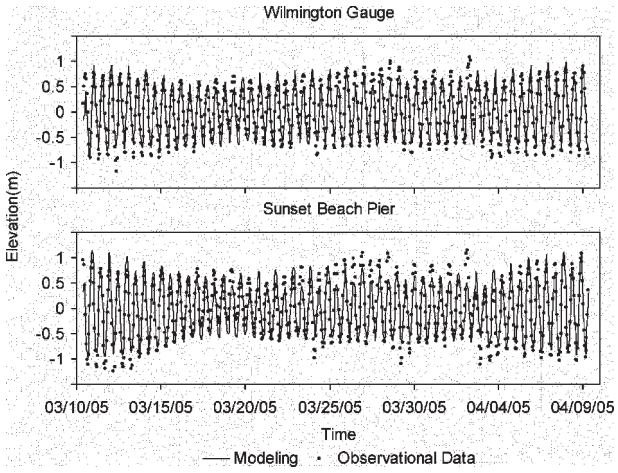

Fig. 2. Comparison between model simulated and observed water level at Wilmington Gauge and Sunset Beach Pier.

Sensitivity Experiments

CFRE Plume Induced by Normal River Discharge

The base case simulation was a plume simulated under the influence of river discharge only (Fig. 4). In the absence of other physical factors such as wind and tidal effects, the plume shows a bulge off the mouth of the CFRE and a narrow coastal current, which propagates towards the west downstream along the North Carolina east-west aligned south coast. This bulge is consistent with the discussion of Chao and Boicourt (1986), Zhang et al. (1987), and Pietrafesa and Janowitz (1988).

We discussed the vertical salinity distribution at the mouth of CFRE (Fig. 1). As shown in Fig. 5, the vertical salinity distribution shows a strong stratification due to freshwater discharge. The depth of the plume changed with bathymetry. The salinity gradient varies greatly in the plume region while its

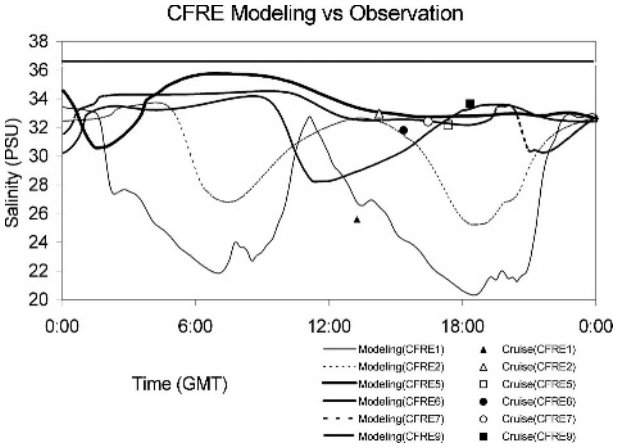

Fig. 3. Comparison between the simulated and observed salinity.

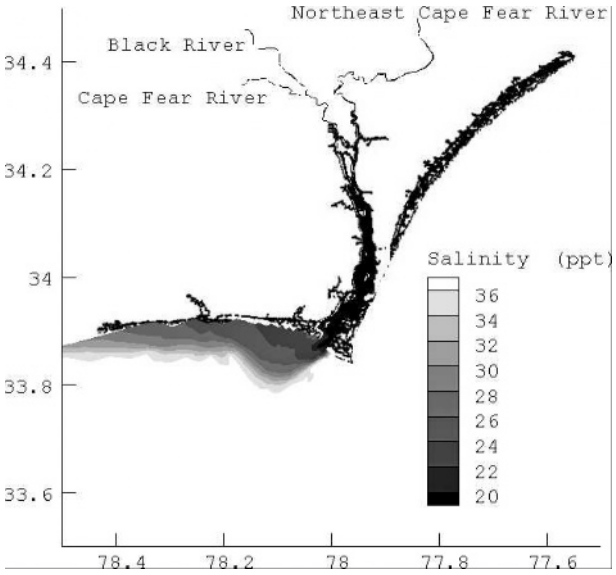

Fig. 4. The sea surface salinity fields forced by normal river discharge after 5 days.

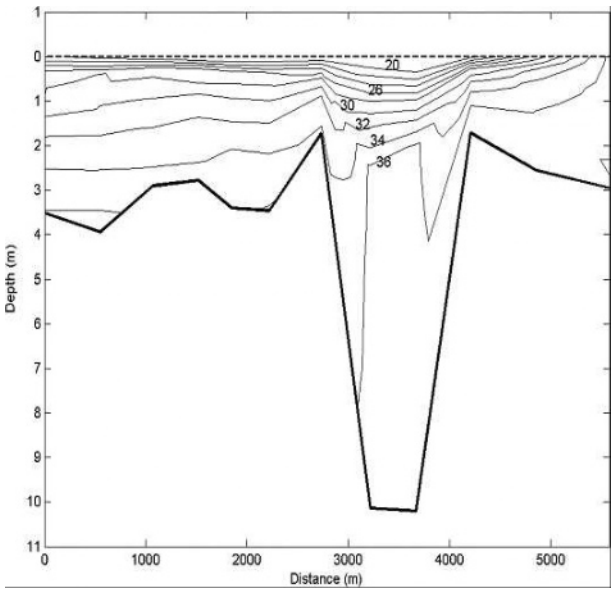

Fig. 5. The vertical salinity fields forced by normal river discharge after 5 days.

changes are smaller outside the plume region. Under the average freshwater discharge effect, low salinity water is only limited to a portion of the surface water. The vertical plume distribution is constricted to the upper 2 or 3 m at the mouth of CFRE and coastal ocean.

Response to Normal River Discharge and 5 m s^{-1} Wind Speeds Under Different Wind Directions

Winds are omni-present in the CFRE region (Pietrafesa et al. 1986), so it is important to include wind effects in plume modeling. We first consider how wind directions influence the plume structure during upwelling (westerly or easterly winds) and downwelling (easterly or westerly winds) events. In all simulations, each river discharge is set to its daily average value and the wind speed is set to 5 m s^{-1}. Easterly downwelling favorable winds will push the plume along the coast to the west of the mouth of the CFRE, and the plume hugs the southern coast (Fig. 6). Under a southwesterly upwelling favorable wind, the plume turns to the left to the east and this upwelling-favorable wind keeps the plume away from the coast. The southwesterly wind driven plume could breech Frying Pan Shoals and enter Onslow Bay as discussed previously by Singer et al. (1980). We see that the surface plume structure is much different under the opposing cases of downwelling versus upwelling winds. By comparing the plume structure with and without wind effects (Figs. 6 and 4), we find that the surface CFRE plume size is reduced and the plume bulge is distorted due to surface mixing under wind conditions.

We next consider how different wind directions influence the vertical structure of the plume, and how the wind cases compare to the no-wind case, as shown in Figs. 5 and 7. In the simulation with wind, the surface salinity value is higher, while the salinity of deeper water is reduced due to the effect of wind-induced vertical mixing. The stratification is a little weaker and the depth of the vertical plume is deeper compared to the situation without winds. The plume depth reaches 4 m under southwesterly upwelling favorable wind, which is deeper than those without wind effects. The vertical plume structure varies under different wind directions, although the change is not as dramatic as that of the surface plume structure. Vertical mixing is strong throughout the entire channel under the case of southwesterly winds, while in the case of easterly wind the mixing is stronger in the left part of the channel (Fig. 7). Southwesterly winds also resulted in a deeper plume than those under other wind directions.

The bottom structure of salinity at the mouth of CFRE is nearly the same under the various wind conditions and was marginally influenced by weak or moderate winds. There is a critical depth beyond which mixing induced by winds of specific magnitude cannot penetrate. As Hetland (2005) pointed out, wind forcing does not affect bottom salinity when the plume has reached its critical depth, and wind induced turbulent mixing is suppressed after this point. As shown in Fig. 7, this critical salinity depth is determined by the various values of wind stress. The plumes do not make bottom contact in

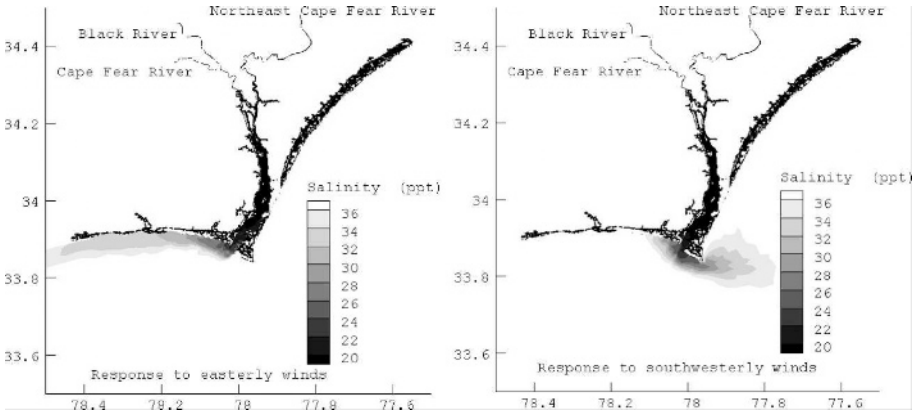

Fig. 6. Surface salinity fields forced by 5 m s^{-1} winds and normal discharge in response to easterly and southwesterly winds.

the deepest water with 5 m s^{-1} wind speeds. This phenomenon is also consistent with the discussions of Berdeal et al. (2002), who suggested that moderate wind forcing will strengthen the surface salinity mixing, while it has little influence on the salinity near the bottom.

Response to Different Wind Speeds Under Southwesterly Winds

The southwesterly wind direction is approximately parallel to the major axis of the estuary and blows offshore. It also dominates this region in the spring (Pietrafesa et al. 1986). We selected the southwesterly wind direction to study the sensitivity of the CFRE plume structure to wind forcing.

As shown in Figs. 6 and 8, the plume size was reduced as the southwesterly wind speed increased from 5 to 20 m s^{-1} due to enhanced surface mixing associated with increased wind speeds. As shown in Figs. 7 and 9, the vertical plume salinity distribution is more uniform as the wind speed and the subsequent vertical mixing increase, while the stratification remains weak. The surface salinity value increases as the wind speed increased from 5 to 20 m s^{-1} under southwesterly winds. This is consistent with the discussion of Berdeal et al. (2002). The plume becomes deeper with decreasing stratification as wind stress increases due to increased vertical mixing.

The bottom salinity value decreases slightly as wind speed increases. The critical salinity depth becomes deeper with increasing wind forcing. The bottom salinity was apparently influenced by the 20 m s^{-1} wind speed. At the same time, the plume's length is much smaller with the increasing wind speed while the depth of the plume increases slightly as shown in Fig. 8. This is consistent with the condition that salt is conserved.

Sensitivity to River Discharge Under the Influence of a Southwesterly Wind

Since southwesterly winds are very common in the CFRE and adjacent ocean (Pietrafesa et al. 1986), we performed simulations of varying discharge with a 5 m s^{-1} southerly wind to study the sensitivity of the CFRE plume. As the river discharge increases

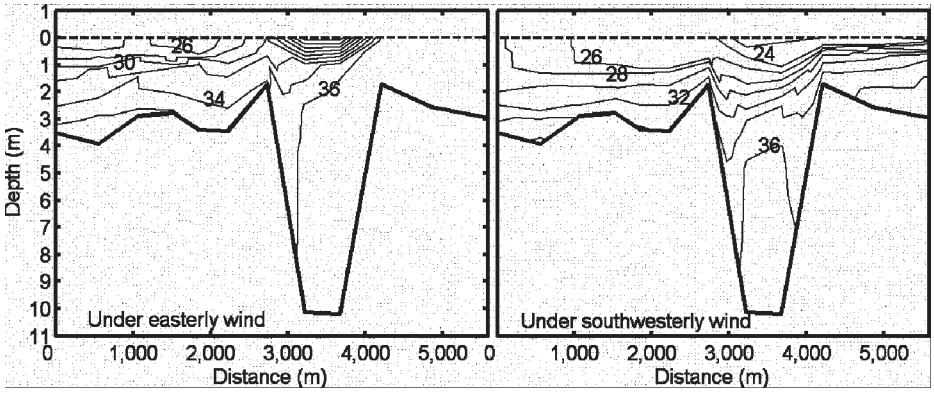

Fig. 7. Vertical salinity fields forced by 5 m s^{-1} winds and normal discharge in response to easterly and southwesterly winds.

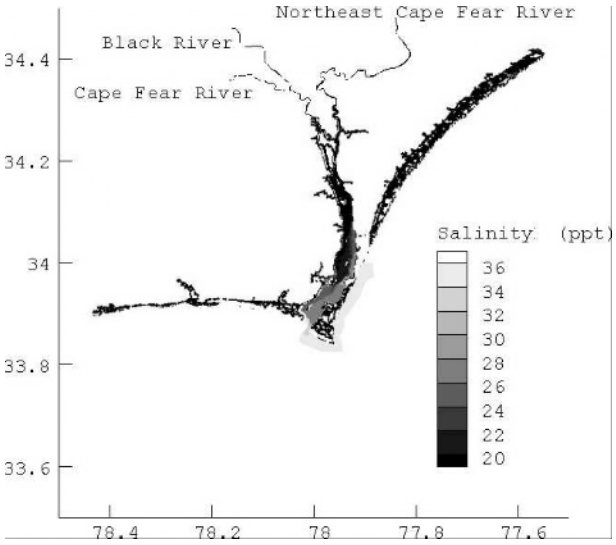

Fig. 8. Plume structure under southwesterly winds and normal river discharge in response to 20 m s^{-1} wind speed.

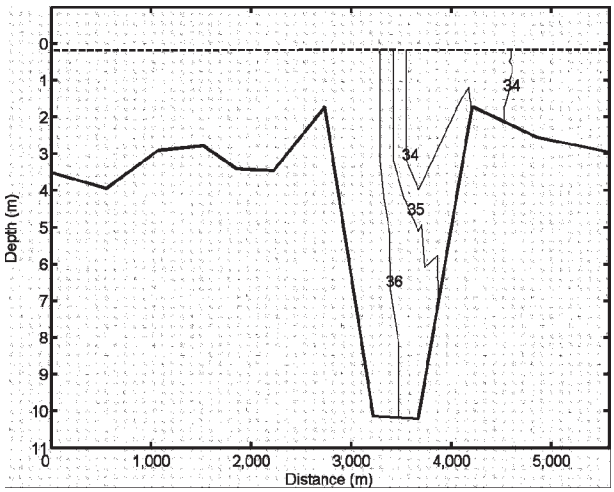

Fig. 9. Vertical salinity fields under southwesterly winds and normal river discharge in response to 20 m s^{-1} wind speed.

from zero to flood conditions, the size of the plume is dramatically increased. There is nearly no plume formation under the no river discharge condition (Fig. 10). The plume remains small under average discharge conditions, while the plume size increases dramatically under relatively high discharge or flood conditions (Figs. 10 and 6).

With the increasing river discharge, the stratification is dramatically increased in the deep water, while the vertical mixing is also increased in the shallow water due to high surface water velocity (Figs. 11 and 7). The vertical plume scale increases with increased river discharge. Even under flooding conditions, high stratification still exists in the deep bottom water, so the surface vertical mixing induced by the river discharge is not as strong as that of wind-induced mixing. The high river discharge could induce the bottom-advected plumes in the shallow water, which was discussed by Yankovsky and Chapman (1997). Higher eddy diffusivity will be induced by the increased discharge (Whitney and Garvine 2006). Unlike the wind induced plume, mixing could deepen the plume depth while shortening the plume length. The strong river discharge will deepen the plume depth and increase the plume length.

Sensitivity to Tidal Effect Under the Influence of Wind and River Discharge

Sensitivity to Tidal Effect Under Normal River Discharge and the Influence of No Winds

The surface salinity distributions were significantly different during high tide and low tide phases (Fig. 12). A dramatic difference in the salinity distribution exists at the mouth of the CFRE, and the along-shelf movements are much weaker compared to the nontidal simulation. At the same time, the surface plume structure is still weaker under low tide conditions compared to the non-tidal conditions (Figs. 12 and 4). The salinity is more than 30 psu with the tidal mixing along the coast, while the surface salinity could reach less than 20 psu without the tidal effect. The strong tidal mixing plus the tidal current weakens the stratification and decreases the surface salinity value.

Based on the vertical plume structures, the stratification is weak under flood tide and low tide (Fig. 13). The plume depth is much deeper compared to the nontidal effect case, where low salinity water could even contact the bottom. Under flood tide phases, there is strong bottom contact. The flooding tide event is strong enough to influence the vertical plume structure, decreasing stratification, and increasing vertical mixing. Under the ebb condition, the plume also has some degree of bottom contact, and stratification is weak. Garvine (2001) and Whitney and Garvine (2006) studied tidally-average vertical salinity distributions using observations and modeling and found that plumes could reach the bottom using the tidally-averaged field, so the modeling results presented here are consistent with their findings.

Compared to the nontidal simulation, the surface salinity is lower during ebb tide and tidal mixing plays a crucial role in the vertical plume structure. The nontidal simulation suggests that the plume makes bottom contact only under flood conditions. Berdeal et al. (2002) mentioned that the plumes do not make bottom contact for the relatively weak wind stress in their simulation since they did not include tidal effects in the model.

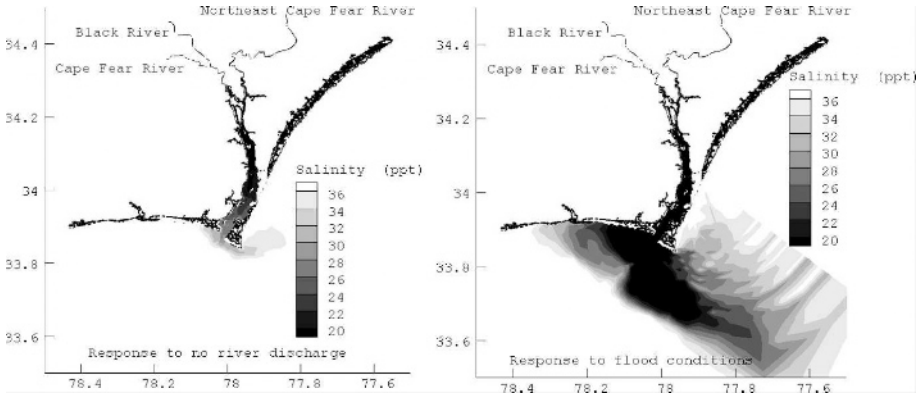

Fig. 10. Surface salinity structure with southwesterly winds of 5 m s^{-1} in response to no river discharge or to flood conditions.

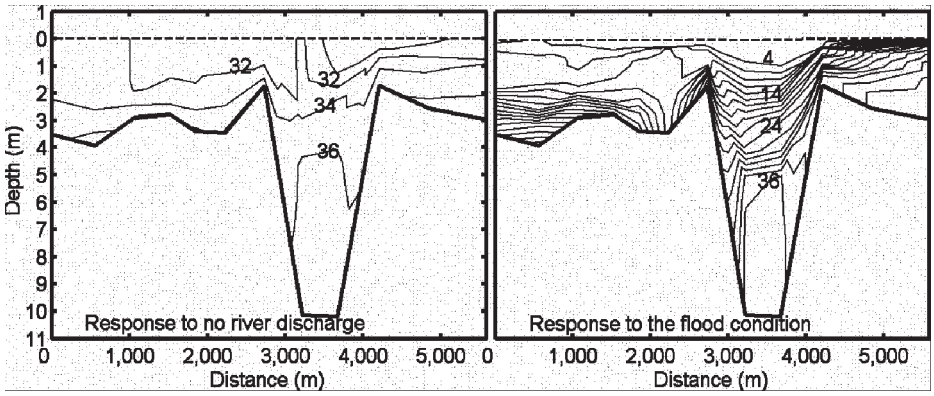

Fig. 11. Vertical salinity structure with southwesterly winds of 5 m s^{-1} in response to no river discharge or to flood conditions.

Sensitivity to Tidal Effect Under Normal River Discharge and the Influence of a Southwesterly Wind

Compared to the nontidal effect, the upshelf and downshelf coastal circulations are weak (Fig. 14). There is no plume formation in either the upshelf or downshelf direction. As in the previous discussions of tidally-driven plumes under no wind effect, the plume size is much smaller during low tide conditions (Fig. 6) and is even smaller during high tide conditions.

From Fig. 15, the distribution of the plume is very similar to that of the no wind scenario. Compared to weak or moderate wind effects, tidal

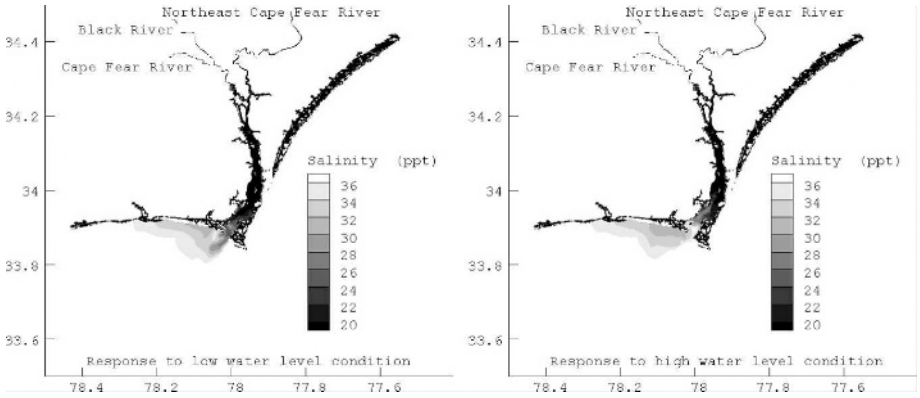

Fig. 12. Plume structure with no wind forcing and normal discharge in response to low or high water level conditions.

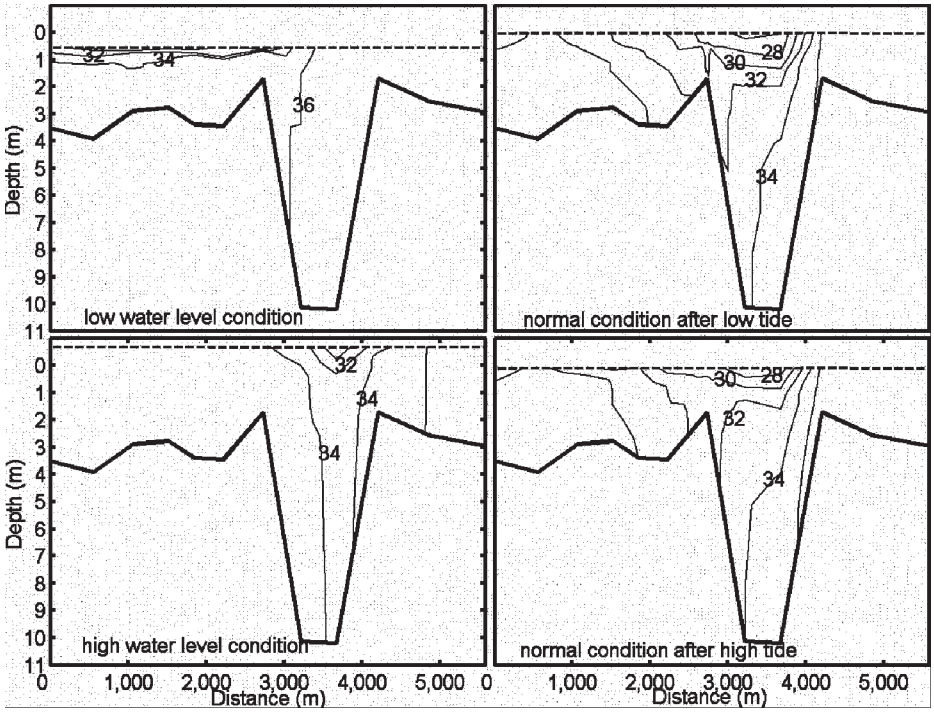

Fig. 13. Plume structure with no wind forcing and normal discharge in response to low water level conditions, normal conditions after low tide, high water level conditions, and normal conditions after the high tide.

mixing plays a crucial role in determining the plume structure.

Discussion

In this study, the three-dimensional EFDC model is configured for the CFRE region to simulate the salinity plume structure. The main conclusions are summarized below.

When average river discharge is imposed without wind effects, the CFRE plume is generally confined to the south-facing coastal shoreline in upper Long Bay and extends in the west direction to form a long narrow trapped structure. For the vertical distribution, low salinity water is only limited to the upper 2 or 3 m at the mouth of CFRE and the coastal ocean.

As the river discharge increased from zero to flood conditions, the size of the surface plume dramatically increased. The high river discharge induced plume could reach shallow water bottoms but not deep water bottoms, and high stratification still exists in the deep bottom water.

The plume's surface structure is significantly different depending on wind directions when the effect of wind is added. Even a moderate wind could fully reverse the buoyancy-driven plume structure in

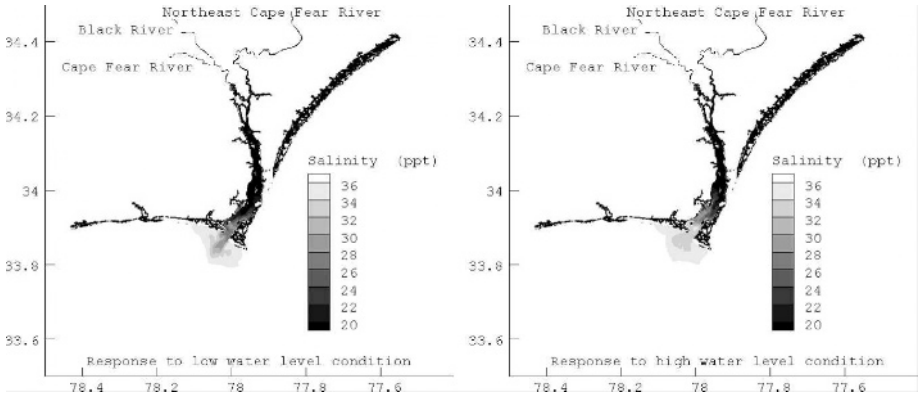

Fig. 14. Plume structure with southwest wind forcing and normal discharge in response to low and high water level conditions.

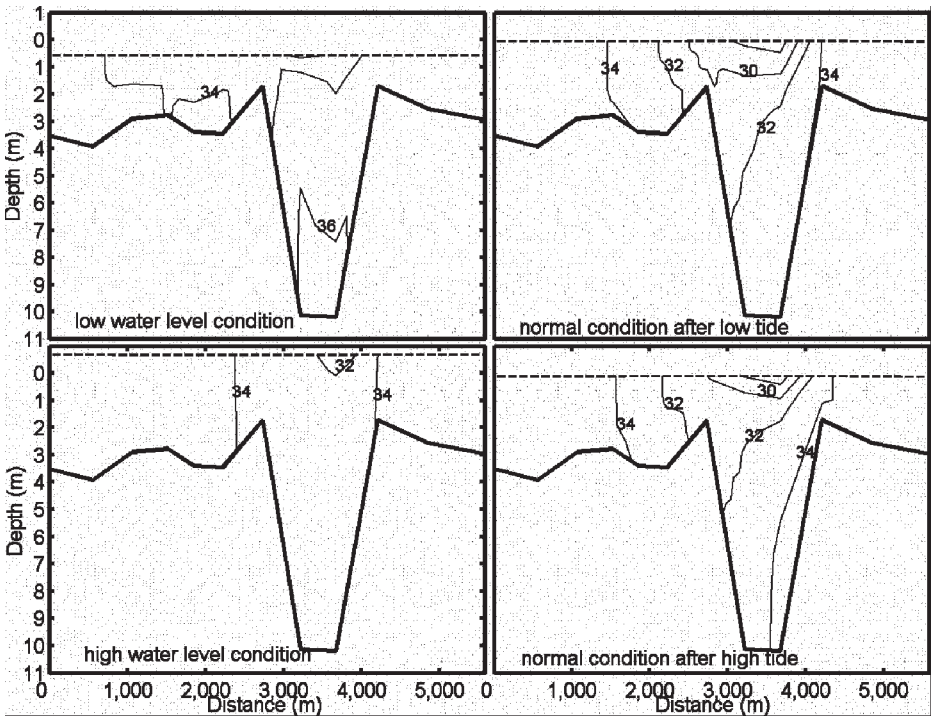

Fig. 15. Plume structure with southwest wind forcing and normal discharge in response to low water level conditions, normal conditions after low tide, high water level conditions, and normal conditions after high tide.

the CFRE under average river discharge conditions. During average river discharge conditions, southwesterly upwelling favorable winds all cause the CFRE plume to depart from the coast to the south of CFRE. Under easterly downwelling favorable winds, the CFRE plume was trapped along the coast under periods of normal river discharge. The surface plume structure is much different under the opposing cases of downwelling versus upwelling winds. The surface plume size was significantly reduced with the increasing wind forcing. Under the strong wind forcing, there is nearly no plume formation at the mouth of CFRE.

Under moderate or weak wind forcing and moderate freshwater discharge, the plume is unlikely to make contact with the bottom given the limitation of the critical salinity depth. There is a very strong stratification in these cases, and the different wind direction could lead to slightly different vertical plume structures. Under strong wind forcing conditions, the stratification is weaker and could cause the vertical salinity distribution to be uniform. The plume also could reach the bottom at the mouth of CFRE.

Astronomical tides are an important factor in influencing the plume's horizontal structure. The plume is extended well offshore in Long Bay during ebb tide whereas the plume reverses into the estuary during flood tide (Fig. 12). Even when the moderate wind effect was included, the plume still showed strong differences during flood tide and ebb tide (Fig. 14). Tidal currents play a key role in influencing the plume's structure in addition to the vertical tidal mixing effect.

Under the effect of tidal mixing, the plume could make bottom contact for most cases, while it seldom makes bottom contact without the tidal effect in the simulation. When compared to the weak or moderate wind effects, tidal mixing plays a crucial role in determining the vertical plume structure.

Frying Pan Shoals, between Long Bay and Onslow Bay, can affect the plume structure by inhibiting a plume from spreading from Long Bay to Onslow Bay. Under flood conditions, the plume region was mostly confined to the Long Bay region (Fig. 10). This is consistent with the discussion of Mallin et al. (2005), which showed that the water mass in Onslow Bay differs greatly from that in Long Bay since very little freshwater enters Onslow Bay from the south. From Fig. 6, it can be seen that some of the plume could breech the Shoals and reach Onslow Bay. This is consistent with the observations of Singer et al. (1980) that shows that under conditions of strong

westerly to southwesterly winds, CFRE plume waters can breach the shoals and have been detected in southern Onslow Bay.

Acknowledgments

This study was supported by the CORMP funded by NOAA under grand award #NA16RP2675 through a subcontract from University of North Carolina at Wilmington. All modeling activities are carried out in the Coastal Fluid Dynamics Lab of North Carolina State University. We thank John Hamrick for providing the source code for the simulations. The authors appreciate the detailed editorial suggestions made by three anonymous reviewers.

Literature Cited

Baptista, A. M., Y. L. Zhang, A. Chawla, M. Zulauf, C. Seaton, E. P. Myers, III, J. Kindle, M. Wilkin, M. Burla, and P. J. Turner. 2005. A cross-scale model for 3D baroclinic circulation in estuary–plume–shelf systems: II. Application to the Columbia River. *Continental Shelf Research* 25:935–972.

Berdeal, I. G., B. M. Hicky, and M. Kawase. 2002. River-forced estuarine plume. *Journal of Physical Oceanography* 18:72–88.

Blumberg, A. F. and G. L. Mellor. 1987. A description of a three-dimensional coastal ocean circulation model, p. 1–16. *In* N. S. Heaps (ed.), Three-dimensional Coastal Ocean Models, Volume 4. American Geophysical Union, Washington, D.C.

Chao, S. Y. 1988. River-forced estuarine plume. *Journal of Physical Oceanography* 18:72–88.

Chao, S. Y. and W. C. Boicourt. 1986. Onset of estuarine plumes. *Journal of Physical Oceanography* 16:2137–2149.

Cheng, R. T. and V. Casulli. 2004. Modeling a three-dimensional river plume over continental shelf using a 3D unstructured grid model, p. 1027–1043. *In* M. L. Spaulding (ed.), Proceedings of the Eighth International Conference on Estuarine and Coastal Modeling, Monterey, California.

Dame, R., M. Alber, D. Allen, M. Mallin, C. Montague, A. Lewitus, A. Chalmers, R. Gardner, C. Gilman, B. Kjerfve, J. Pinckney, and N. Smith. 2000. Estuaries of the south Atlantic coast of North America: Their geographical signatures. *Estuaries* 23:793–819.

Fong, D. A. 1998. Dynamics of freshwater plumes: Observations and numerical modeling of the wind-forced response and alongshore freshwater transport, Ph.D. Dissertation, Massachusetts Institute of Technology/Woods Hole Oceanographic Institution Joint Program in Oceanography, Woods Hole, Massachusetts.

Fong, D. A. and W. R. Geyer. 2002. The alongshore transport of freshwater in a surface-trapped river plume. *Journal of Physical Oceanography* 32:957–972.

Galperin, B., L. H. Kantha, S. Hassid, and A. Rosati. 1988. A quasi-equilibrium turbulent energy model for geophysical flows. *Journal of Atmospheric Science* 45:55–62.

Garvine, R. W. 1987. Estuary plumes and fronts in shelf waters: A layer model. *Journal of Physical Oceanography* 17:1877–1896.

Garvine, R. W. 1999. Penetration of buoyant coastal discharge onto the continental shelf: A numerical model experiment. *Journal of Physical Oceanography* 29:1892–1909.

Garvine, R. W. 2001. The impact of model configuration in studies of buoyant coastal discharge. *Journal of Marine Research* 59:193–225.

Hamrick, J. M. 1992. A Three-Dimensional Environmental Fluid Dynamics Computer Code: Theoretical and Computational Aspects Special Report 317. The College of William and Mary, Virginia Institute of Marine Science, Williamsburg, Virginia.

Hetland, D. R. 2005. Relating river plume structure to vertical mixing. *Journal of Physical Oceanography* 35:1667–1688.

Hickey, B. M., L. J. Pietrafesa, D. A. Jay, and W. C. Boicourt. 1998. The Columbia River plume study: Substantial variability in the velocity and salinity field. *Journal of Geophysical Research* 103:10339–10368.

Ji, Z., M. R. Morton, and J. M. Hamrick. 2001. Wetting and drying simulation of estuarine processes. *Estuarine Coastal and Shelf Science* 53:683–700.

Kourafalou, V. H., T. N. Lee, L. Oey, and J. Wang. 1996b. The fate of river discharge on the continental shelf, 2, Transport of coastal low-salinity waters under realistic wind and tidal forcing. *Journal of Geophysical Research* 101:3435–3456.

Kourafalou, V. H., L. Oey, J. Wang, and T. N. Lee. 1996a. The fate of river discharge on the continental shelf, 1, Modeling the river plume and inner shelf coastal current. *Journal of Geophysical Research* 101:3415–3434.

Mallin, M. A., L. B. Cahoon, and M. J. Durako. 2005. Contrasting food-web support bases for adjoining river-influenced and non-river influenced continental shelf ecosystems. *Estuarine Coastal and Shelf Science* 62:55–62.

Mellor, G. L. and T. Yamada. 1982. Formation of a turbulent closure model for geophysical fluid problems. *Revista Geophysical Space Physics* 20:851–875.

O'Donnell, J. 1990. The formation and fate of a river plume: A numerical model. *Journal of Physical Oceanography* 20:551–569.

Park, K., H. Jung, H. Kim, and S. Ahn. 2005. Three-dimensional hydrodynamic-eutrophication model (HEM-3D): Application to Kwang-Yang Bay, Korea. *Marine Environmental Research* 60:171–193.

Pietrafesa, L. J. and G. S. Janowitz. 1988. Physical oceanographic processes affecting larval transport around and through North Carolina inlets. *American Fisheries Society* 3:34–50.

Pietrafesa, L. J., G. S. Janowitz, T. Y. Chao, R. H. Weisberg, F. Askari, and E. Noble. 1986. The physical oceanography of the Pamlico Sound. University of North Carolina Sea Grant Publication UNC-WP-86-5, Raleigh, North Carolina.

Shen, J. and L. Haas. 2004. Calculating age and residence time in the tidal York River using three-dimensional model experiments. *Estuarine, Coastal and Shelf Science* 61:449–461.

Sheng, J. 2001. Dynamics of a buoyancy-driven coastal jet: The Gaspe Current. *Journal of Physical Oceanography* 31:3146–3163.

Singer, J., L. Atkinson, and L. J. Pietrafesa. 1980. Summertime advection of low salinity surface water into Onslow bay. *Estuarine and Coastal Marine Science* II:73–82.

Walker, N. D., W. J. Wiseman, L. J. Rouse, and A. Babin. 2005. Effects of river discharge, wind stress, and slope eddies on circulation and the satellite-observed structure of the Mississippi river plume. *Journal of Coastal Research* 21:1228–1244.

Whitney, M. M. and R. W. Garvine. 2006. Simulating the Delaware bay buoyant outflow: Comparison with observations. *Journal of Physical Oceanography* 36:3–21.

Wu, J. 1982. Wind-stress coefficients over sea surface from breeze to hurricane. *Journal of Geophysical Research* 87:9704–9706.

Xia, M., L. Xie, and L. J. Pietrafesa. 2006. Cape Fear River Estuary plume modeling: Model configuration and sensitivity experiments, p. 66–84. *In* M. L. Spaulding (ed.), Proceedings of the Ninth International Conference on Estuarine and Coastal Modeling, Charleston, South Carolina.

Xie, L. and L. J. Pietrafesa. 1999. System wide modeling of wind and density driven circulation in the Croatan-Albemarle Pamlico estuary system. Part I: Model configuration and testing. *Journal of Coastal Research* 15:1163–1177.

Xing, J. X. and A. M. Davies. 1999. The effect of wind direction and mixing upon the spreading of a buoyant plume in a non-tidal regime. *Continental Shelf Research* 19:1437–1483.

YANG, Z. AND J. M. HAMRICK. 2005. Optimal control of salinity boundary condition in a tidal model using a variational inverse method. *Estuarine Coastal and Shelf Science* 62:13–24.

YANKOVSKY, A. E. AND D. C. CHAPMAN. 1997. A simple theory for the fate of buoyant coastal discharges. *Journal of Physical Oceanography* 27:1386–1401.

ZHANG, Q. H., G. S. JANOWITZ, AND L. J. PIETRAFESA. 1987. The interaction of estuarine and shelf waters: A model and applications. *Journal of Physical Oceanography* 17:455–469.

Received, November 15, 2006
Revised, March 6, 2007
Accepted, March 22, 2007